Vibrational Circular Dichroism of Polypeptides. 7. Film and Solution Studies of β-Sheet-Forming Homooligopeptides§

U. Narayanan,† T. A. Keiderling,*† G. M. Bonora,‡ and C. Toniolo*‡

Contribution from the Department of Chemistry, University of Illinois at Chicago, Chicago, Illinois 60680, and Centro di Studio sui Biopolimeri del CNR, Dipartimento di Chimica Organica, Università di Padova, 35131 Padova, Italy. *Received August 30, 1985*

Abstract: Vibrational circular dichroism (VCD) of films of monodispersed, terminally blocked, linear homooligopeptides of L-Nva, L-Val, and L-Leu up to $n = 7$ have been measured in the amide I and A regions and compared to previously reported data on $(L\text{-Ala})_n$ oligomers. All except Leu show a maximum in the $\Delta A/A$ value, which occurs at a higher n value than that previously assigned to the onset of β-structure. This is indicative of two structural transitions, the second one of which may be due to formation of a fully developed β-type structure. The data imply that the nature of the side-chain group correlates with the observed tendency to form a stable β-structure: Ala > Val ≃ Nva > Leu. VCD was also obtained for Boc-$(L\text{-Val})_7$-OMe, Boc-$(D\text{-Ala})_7$-OMe, and Boc-$(L\text{-Ala})_6$-OMe in TFE solution. These are the first reports of solution-phase oligopeptide β-structure VCD. The dependence of the VCD intensity on temperature and solvent (TFE/HFIP) can be interpreted as there being a gradual transition between two structures in solution. This work definitively points out the inadequacies of using IR absorption frequencies to determine the detailed nature of peptide secondary structure and to obtain a complete picture of structural changes.

Vibrational circular dichroism (VCD), the measurement of the differential absorbance of left and right circularly polarized light by molecular vibrations in the infrared (IR) region, is a new technique of much promise for stereochemical analysis.[1-5] In recent years, we and others have shown that such measurements can also be applied to polypeptide systems to yield conformationally sensitive information.[6-11] VCD for solution-phase α-helical molecules has shown a consistent pattern in the amide A, I, and II regions that appears to correlate to the helix-screw sense.[6-8,11] Solution VCD for β-sheets has not been previously described, but we have reported film data for several polypeptides[9] and a series of homooligopeptides of L-Ala.[10]

These film studies have shown that β-sheet polypeptides give rise to a somewhat systematic pattern of VCD signals in these regions. However, the sign and shape observed for the bands in films appear to vary with the nature of the amino acid component.[9] It is felt that the film structure gives rise to additional effects beyond the interchain hydrogen bonding considered in available theoretical models of polypeptide VCD.[12,13] Additionally, scattering effects such as those seen in the VCD of liquid crystals may be operative.[14] For this reason and at this time, film VCD can be used only as an empirical tool for studying conformational change and is best limited to comparing systems under conditions that are as consistent as possible.

It is such an application of VCD that we reported for Boc-$(L\text{-Ala})_n$-OMe, $n = 3$-7, homooligopeptides.[10] In that study, it was seen that the $\Delta A/A$ value went through two distinct changes as n increased. The first, a sharp increase in $\Delta A/A$, coincided with the shift in the amide I absorption maximum from ~1650 to ~1630 cm^{-1} that is traditionally taken as a marker for the onset of β-structure.[15-19] The second change occurred at a higher n value and represented a decrease in $\Delta A/A$ toward a value approaching that which was found for polypeptides thought to have β-sheet structures.[9] We attributed this second change to the formation of a fully developed β-structure in the longer blocked $(L\text{-Ala})_n$ homooligopeptides that had not previously been detected.

It is important to test the generality of these results and, in particular, to see if homooligopeptides based on other amino acids also go through a $\Delta A/A$ maximum or if that is unique to those derived from L-Ala. Additionally, it is important to know to what extent film VCD data correlate to solution results. Unlike for most β-structure-forming polypeptides, there are reports of solution-phase IR absorption measurements for some β-forming oligopeptides.[16,18,19]

In recent years, a series of studies have been carried out in the Padova laboratory to analyze the solid-state conformational preferences of monodispersed, N- and C-protected, linear homooligopeptides.[15-17,19-22] Emphasis has been on oligomers of aliphatic side-chain amino acids (e.g, L-Ala, L-Val, L-Nva, and L-Leu oligomers to the heptamers) by using inter alia vacuum-ultraviolet CD (VUV CD) and IR absorption spectroscopies. Spectra characteristic of β-structure were found for the higher members of all the series examined. In this paper, film VCD of the $(L\text{-Val})_n$, $(L\text{-Leu})_n$, and $(L\text{-Nva})_n$ series are reported and compared to the earlier L-Ala oligomer results.[10] Additionally, we have obtained the first solution-phase β-structure VCD for the $(L\text{-Val})_7$, $(L\text{-Ala})_6$, and $(D\text{-Ala})_7$ oligomers and will discuss their temperature and solvent dependencies in relationship to the film data presented here and previously.[10]

† University of Illinois at Chicago.
‡ Università di Padova.
§ Part 6: Yasui, S. C.; Keiderling, T. A. *Biopolymers* **1986**, *25*, 5-15.

(1) Keiderling, T. A. *Appl. Spectrosc. Rev.* **1981**, *17*, 189-226.
(2) Nafie, L. A. *Vib. Spectra Struct.* **1981**, *10*, 153-226.
(3) Mason, S. F., *Adv. Infrared Raman Spectrosc.* **1980**, *8*, 282-321.
(4) Stephens, P. J.; Clark, R. In *Optical Activity and Chiral Discrimination*; Mason, S. F., Ed.; Reidel: Dordrecht, The Netherlands, 1979; pp 263-287.
(5) Nafie, L. A. *Adv. Infrared Raman Spectrosc.* **1984**, *11*, 49-93.
(6) Singh, R. D.; Keiderling, T. A. *Biopolymers* **1981**, *20*, 237-240.
(7) Lal, B. B.; Nafie, L. A. *Biopolymers* **1982**, *21*, 2161-2183.
(8) Sen, A. C.; Keiderling, T. A. *Biopolymers* **1984**, *23*, 1519-1532.
(9) Sen, A. C.; Keiderling, T. A. *Biopolymers* **1984**, *23*, 1533-1545.
(10) Narayanan, U.; Keiderling, T. A.; Bonora, G. M.; Toniolo, C. *Biopolymers* **1985**, *24*, 1257-1263.
(11) Yasui, S. C.; Keiderling, T. A.; Bonora, G. M.; Toniolo, C. *Biopolymers* **1986**, *25*, 79-89.
(12) Schellman, J. A.; Becktel, W. J. Biopolymers **1983**, *22*, 171-187.
(13) Snir, J.; Frankel, R. A.; Schellman, J. A. *Biopolymers* **1975**, *14*, 173-196.
(14) Korte, E. H.; Schrader, B. *Adv. Infrared Raman Spectrosc.* **1981**, *8*, 226-282.
(15) Baron, M. H.; DeLozé, C.; Toniolo, C.; Fasman, G. D. *Biopolymers* **1979**, *18*, 411-424.
(16) Palumbo, M.; DaRin, S.; Bonora, G. M.; Toniolo, C. *Makromol. Chem.* **1976**, *177*, 1477-1492.
(17) Toniolo, C.; Palumbo, M. *Biopolymers* **1977**, *16*, 219-224.
(18) Baron, M. H.; DeLozé, C.; Toniolo, C.; Fasman, G. D. *Biopolymers* **1978**, *17*, 2225-2239.
(19) Bonora, G. M.; Palumbo, M.; Toniolo, C.; Mutter, M. *Makromol. Chem.* **1979**, *180*, 1293-1304.
(20) Balcerski, J. S.; Pysh, E. S.; Bonora, G. M.; Toniolo, C. *J. Am. Chem. Soc.* **1976**, *98*, 3470-3473.
(21) Kelly, M. M.; Pysh, E. S.; Bonora, G. M.; Toniolo, C. *J. Am. Chem. Soc.* **1977**, *99*, 3264-3266.
(22) Del Pra, A.; Toniolo, C. *Macromolecules* **1978**, *11*, 793-797.

0002-7863/86/1508-2431$01.50/0

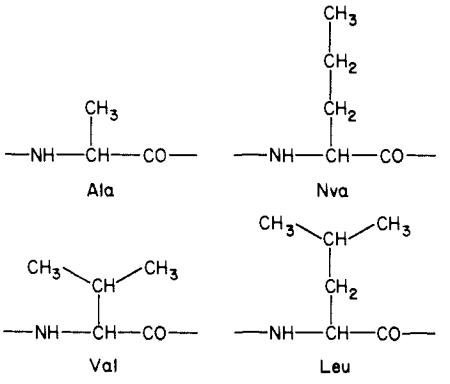

Experimental Section

The homooligopeptides Boc-(L-Val)$_n$-OMe, Boc-(L-Leu)$_n$-OMe, and Boc-(L-Nva)$_n$-OMe, n = 2–7, as well as Boc-(L-Ala)$_6$-OMe and Boc-(D-Ala)$_7$-OMe were all synthesized in the Padova laboratory by methods previously reported.[23-27] VCD and IR absorption spectra presented here were measured under identical conditions on the UIC instrument, which also has been previously described in detail.[1] The film samples were prepared by precipitation from a 2,2,2-trifluoroethanol (TFE) solution at room temperature onto a 2-mm-thick CaF_2 window that was placed in a fume hood to provide constant air flow over the sample. To improve optical homogeneity of the film, the sample was constantly rotated during film deposition by using a conventional magnetic stirrer coupled to a solvent and window holder of our own design. Films were tested for satisfactory VCD characteristics by comparison of the film VCD obtained with the sample placed at different angles about the light beam axis. Those giving position-dependent spectra were redissolved for another attempt. For all data reported here, the sign and peak-to-peak magnitude of $\Delta A/A$ were consistent with rotational position to within $\simeq$20%. All data were rechecked at least once more by preparing a new film with a generally different absorbance. In these latter cases, the band shapes were consistent but, with two exceptions, the magnitudes varied by up to a factor of 2. This is significantly worse sample-to-sample agreement than that found for the (L-Ala)$_n$ series.[10]

All samples used were prepared with absorbances between 0.1 and 0.9, and the VCD spectra presented in the figures, in particular, are derived from samples with absorbances between 0.15 and 0.35. For very low absorbance (i.e., less than 0.10), our measurements are sometimes subject to considerable error due to noise; with very high absorbance (i.e., greater than 1.0), the resulting film thickness and transmittance minimum may cause artifacts. For comparison of different systems, it is best to have film data collected from samples of approximately the same absorption. The film VCD measurements were done with $\simeq$11-cm^{-1} resolution and a 10-s time constant in the amide I and $\simeq$14 cm^{-1} and 3 s, respectively, in the amide A region. Two to four scans were averaged and corrected by subtraction of a VCD base line obtained from a similarly prepared poly(Gly)$_n$ film run under the same experimental conditions. In most cases the films gave VCD of large enough magnitudes that the details of base-line correction proved to be unimportant for improving flatness. However, individual films did cause a shift from zero or, sometimes, a curve of the overall base line, which we have attempted to correct by subsequent digital offset.

We had difficulty obtaining satisfactory films for VCD of all the dimers and trimers due to their tendency to deposit unevenly as granules on the CaF_2 window. It was also difficult to prepare films of (L-Leu)$_4$ and (L-Val)$_4$. For (L-Val)$_4$ only films with $A \sim 1$ gave reproducible VCD results, and no reliable (L-Leu)$_4$ VCD was obtained.

The film VCD and IR absorption data are presented in terms of ΔA and A because the film thickness varies and the concentrations are difficult to properly evaluate. In the figures, ΔA and A for a given sample are scaled from the actual 0.15–0.35 to an absorbance maximum of 1 for ease of visual comparison of the $\Delta A/A$ results.

Solution samples of the heptamers of L-Leu, L-Val, L-Nva, and D-Ala and of the hexamer of L-Ala were made by preparing concentrated solutions in TFE. Unfortunately, we did not obtain saturation for (L-Leu)$_7$ and (L-Nva)$_7$, and the resulting IR spectra indicated a randomly coiled structure. The L-Val and D-Ala heptamers generally took 2–3 days to form a saturated, viscous, cloudy solution, but (L-Ala)$_6$ took just 1 h or so. These solutions were filtered through loosely packed glass wool to remove visible solute particles; then, a drop or so of solvent was added, slightly unsaturating the solution, to prevent precipitation during the measurements. The resulting solutions still had a cloudy appearance. Some initial preparations were clear but later proved to be significantly unsaturated. Solutions of (L-Val)$_7$ and (L-Ala)$_6$ were also prepared in mixtures of TFE and 1,1,1,3,3,3-hexafluoropropan-2-ol (HFIP) with the percent of HFIP being nominally (by volume) 0, 10, 20, 30, and 33. The procedure for making these mixed-solvent samples was the same as above. An alternate test was made by adding a concentrated HFIP solution to a saturated TFE solution. This alternate method did not work as well as the use of premixed solvent because the HFIP could not be saturated with the available (L-Val)$_7$ sample. Unfortunately, insufficient amounts of (D-Ala)$_7$ were available for a parallel solvent composition study.

The absorption and VCD spectra were measured in a cell consisting of two CaF_2 windows separated by a Teflon spacer. The spectra were run shortly after the filtration step. Allowing the solution to stand for longer periods of time generally resulted in a loss of VCD signal and the appearance of precipitate. The degradation time also varied with the sample. For example, the absorption and VCD spectra of (D-Ala)$_7$ (in the amide I region) slowly decreased over 1 week and disappeared thereafter. On the other hand, the (L-Val)$_7$ solution exhibited qualitatively the same VCD even after 1 month or more; however, unless the sample was sealed under N_2, an additional IR absorption band grew in at 1720 cm^{-1} after a few weeks, presumably due to H_2O. Additionally, more dilute solutions seemed to be less stable in terms of VCD; for (L-Ala)$_6$ the lifetime was as short as hours.

For the solution experiments, the ϵ and $\Delta\epsilon$ values reported are determined indirectly by evaporating a known volume of solution and determining the residual weight that then leads to determination of the concentration. These should be good to $\pm$10%, but the error will clearly depend on the amount of solution available.

For the temperature study, solutions of (L-Val)$_7$ in TFE were prepared as described above. A small amount of solvent was added to lower the concentration below saturation to 2×10^{-3} M. The solution remained cloudy and gave the expected β-sheet amide I band in absorption. The sample cell, consisting of two CaF_2 windows and a 0.20-mm Teflon spacer, was filled and mounted in a brass holder having a jacket through which water was circulated from a thermostated bath.[28] Transmittance was also measured at all temperatures to monitor sample changes. The original signal was recovered upon cooling back to room temperature so that the process appeared to be fully reversible. The VCD base line appeared to shift as a function of temperature, presumably due to strain in the cell. This effect was much smaller than the overall temperature effect so that the qualitative trends reported here are not adversely affected.

For these solution studies, in the amide I region, a resolution of $\sim$14 cm^{-1} and a time constant of 30 s were used for the best VCD determinations, with four to six scans being averaged. The base line used is a mixture of acetophenone, methyl acetate, and methyl acrylate in TFE prepared to match the oligopeptide absorbances as closely as possible. The resultant VCD proved to be relatively insensitive to the nature of the base-line sample due to the large signals measured, i.e., just solvent gave results about as good. For the temperature- and solvent-dependent studies, a 10-s time constant was used and only two scans were averaged. Absorbance scans of these solution samples show excess noise due to low transmission of the solvent system and interfering water vapor absorptions.

Results

Most of the experiments described above led to reproducible, easily detected VCD. The films, as noted in our polypeptide work,[9] gave more intense signals than did the solutions, but the major problem in measuring VCD of the latter was stability with time and not signal size. Below, we first describe our film results, which can be compared to the (L-Ala)$_n$ film results previously published,[10] and then detail our various solution studies.

Film Studies. In general, these studies of (L-Val)$_n$, (L-Leu)$_n$, and (L-Nva)$_n$ were more difficult than the (L-Ala)$_n$ work because the films proved harder to prepare under the constraint that the VCD be orientation free. Probably, as a consequence, the film-to-film variation in amplitude was also much greater for these oligomers (typically less than a factor of 2) than for (L-Ala)$_n$

(23) Toniolo, C.; Bonora, G. M.; Fontana, A. *Int. J. Pept. Protein Res.* **1974**, *6*, 371–380.
(24) Bonora, G. M.; Maglione, A.; Toniolo, C. *Polymer* **1974**, *15*, 767–770.
(25) Bonora, G. M.; Maglione, A.; Fontana, C.; Toniolo, C. *Bull. Soc. Chim. Belg.* **1975**, *84*, 299–304.
(26) Bonora, G. M.; Nisato, D.; Toniolo, C. *Makromol. Chem.* **1975**, *176*, 2535–2545.
(27) Toniolo, C.; Bonora, G. M. *J. Polym. Sci., Polym. Chem. Ed.* **1976**, *14*, 515–518.
(28) Narayanan, U. Ph.D. Thesis, University of Illinois at Chicago, 1986.

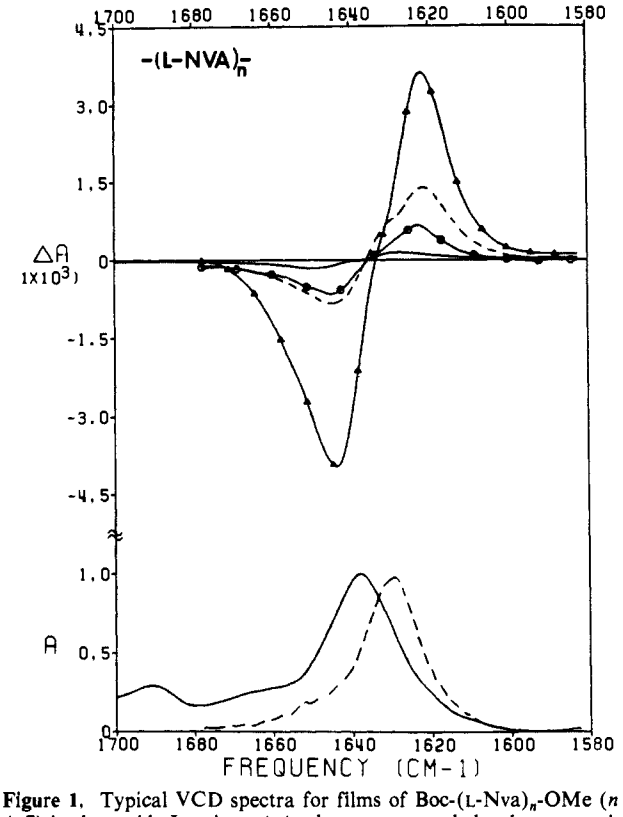

Figure 1. Typical VCD spectra for films of Boc-(L-Nva)$_n$-OMe (n = 4–7) in the amide I region. ΔA values were rescaled to be appropriate for a maximum A = 1. Actual absorbances were ~0.3. Normalized absorption spectra for n = 4 and 7 only are shown for comparison. Data were obtained with a resolution of ≃11 cm^{-1}, at a time constant of 10 s, and by averaging two to four scans. Symbols: n = 4 (—), 5 (○), 6 (△), 7 (---).

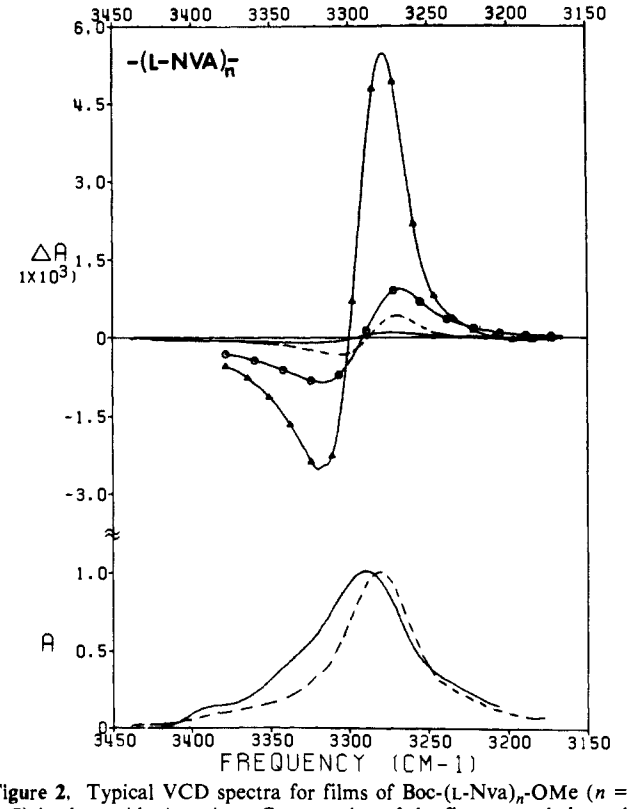

Figure 2. Typical VCD spectra for films of Boc-(L-Nva)$_n$-OMe (n = 4–7) in the amide A region. Construction of the figure, symbols, and spectral details are the same as in Figure 1. Actual absorbances varied from 0.15 to 0.35 for different samples. Data were obtained with a resolution of ≃14 cm^{-1}, at a time constant of 3 s, and by averaging two to four scans. Absorption spectra for n = 4 and 7 only are shown for comparison.

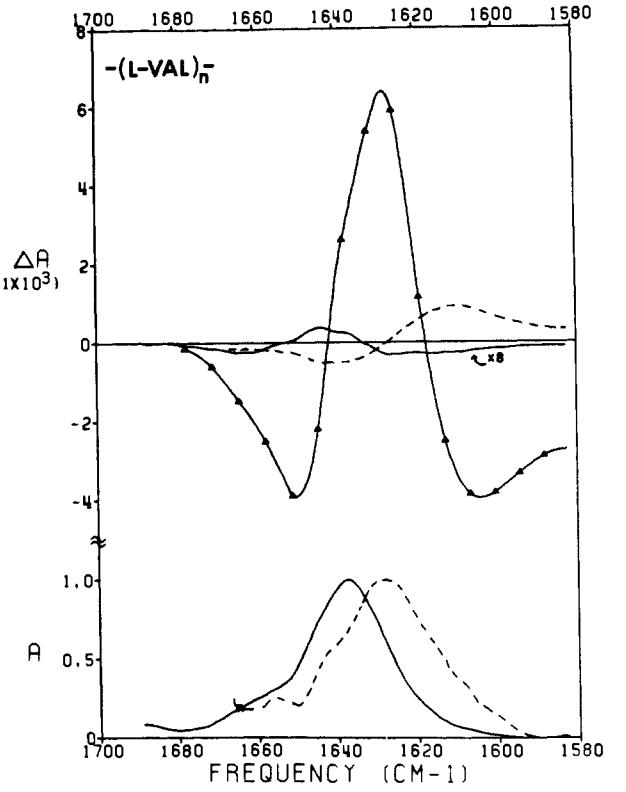

Figure 3. Typical VCD spectra for films of Boc-(L-Val)$_n$-OMe (n = 5–7). Construction of the figure and spectral details are the same as in Figure 1. Normalized absorption spectra for n = 5 and 7 only are shown for comparison. Symbols: n = 5 (—), 6 (△), 7 (---). n = 5 is expanded by 8 for visibility above the base line.

(≲25%). Measurements were made in both the amide A and amide I regions, but those for the amide I proved to be the most reliable and gave variations most easily seen as sensitive to change in n value. The effective range of available oligomer lengths was limited in that n = 2 and n = 3 oligomers did not give reliable films for any of these series.

(L-**Nva**)$_n$ oligomer samples gave the most consistent results and the longest series (in terms of n) of good-quality films. Normalized (L-Nva)$_n$ amide I VCD for n = 4–7 are shown in Figure 1. As in the (L-Ala)$_n$ results, the zero crossing of the sigmoidal VCD curve parallels the decrease in frequency with increasing n found for the absorption maximum and, within experimental error, lies at almost the same value. The VCD magnitude, as measured by the peak-to-peak excursion of $\Delta A/A$, again as for (L-Ala)$_n$, goes through a maximum with increasing n. Here, a sharp rise is noted between n = 4 and 6, and a decrease starts between n = 6 and 7. These changes occur at somewhat higher n values than for (L-Ala)$_n$. It is not clear that a final, stable level of $\Delta A/A$ has been reached by n = 7. The bandwidths appear to be consistent for n = 4–7 whereas for (D-Ala)$_7$ a significant decrease was noted compared to n = 3–6.[10] Additionally, the $\Delta A/A$ value for n = 4 is very small and implies that shorter lengths might yield effectively zero VCD. Virtually the same pattern in $\Delta A/A$ is found for the amide A (Figure 2), with n = 6 being a peak value and n = 4 being very small.

(L-**Val**)$_n$ oligomers yielded somewhat different results from (L-Nva)$_n$ and (L-Ala)$_n$. First of all, the amide I VCD line shapes for n = 4–6 have three extrema (–, +, –) (Figure 3) rather than the simple bisignate pattern seen in the other two cases. Hence, the zero crossings give a much less useful measure of change with n than before. After repeated attempts at its preparation, the n = 4 oligomer gave only two films with measurable VCD, and these both had an absorbance of 1.0. Also, the n = 6 result varied over a factor of 3 in $\Delta A/A$ for the amide I. No trends in line width were apparent.

The trend in $\Delta A/A$ values for the amide I bands goes though a maximum at n = 6, as was found for (L-Nva)$_n$; however, the

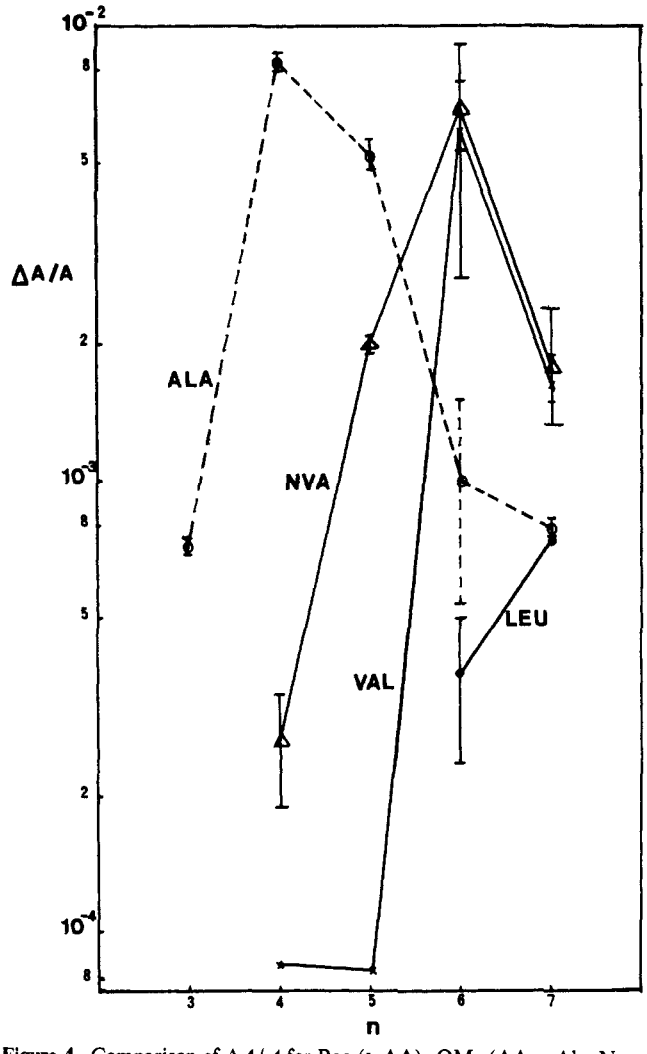

Figure 4. Comparison of $\Delta A/A$ for Boc-(L-AA)$_n$-OMe (AA = Ala, Nva, Val, Leu; n = 3-7) in the amide I region. Symbols: Ala (○), Nva (△), Val (×), Leu (●).

n = 5 values are much smaller than the n = 6 values as compared to those for the (L-Nva)$_n$ case. This gives the appearance of a transition tending to occur at higher n, which would correlate with the trends previously noted on the basis of VUV CD line shape and IR absorption maximum measurements.[16,19,20] This impression is further emphasized by the fact that in the amide A region we were not able to detect significant VCD for n = 4 or 5 but that n = 6 gave significantly larger $\Delta A/A$ than did n = 7.

(L-**Leu**)$_n$ gave the fewest samples with measurable VCD. Only for n = 6 and 7 could we definitely say that amide I VCD was detectable; in these cases, n = 7 gave somewhat larger but still quite small signals. Clearly, no implications as to two structural transitions paralleling those of the previously discussed systems can be drawn for (L-Leu)$_n$. However, to the extent that the data are parallel, one must conclude that the first transition occurs at higher n in (L-Leu)$_n$ than in the other oligomers we have studied. In the amide A region, n = 5 gave VCD of magnitude greater than or comparable to that of n = 6, but this corresponds to *very* broad absorption as compared to that obtained with n = 6 and n = 7.

Summary. The trends in $\Delta A/A$ vs. n for the amide I are compared in Figure 4 for these three series of oligomers described above along with the previously reported data for (L-Ala)$_n$. A parallel comparison for the frequency of the corresponding absorption maximum is shown in Figure 5. A clear shift to higher values of n for the initial rise in $\Delta A/A$ and, as appropriate, for the subsequent fall is clearly evident in the order Ala < Val ≅ Nva < Leu. A similar plot for the amide A offers no additional information.

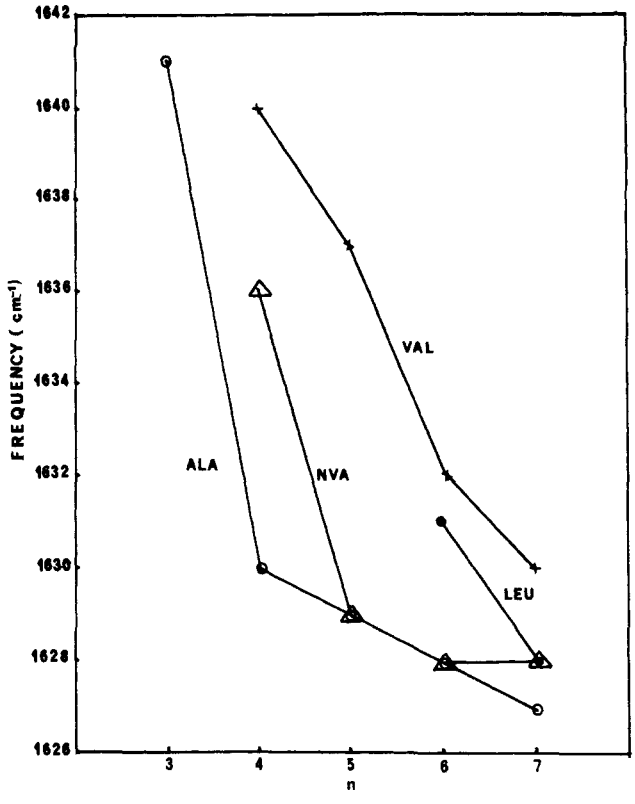

Figure 5. Comparison of the frequency of the absorbance maximum for films of Boc-(L-AA)$_n$-OMe (AA = Ala, Nva, Val, Leu; n = 3-7) in the amide I region. Symbols used are the same as in Figure 4.

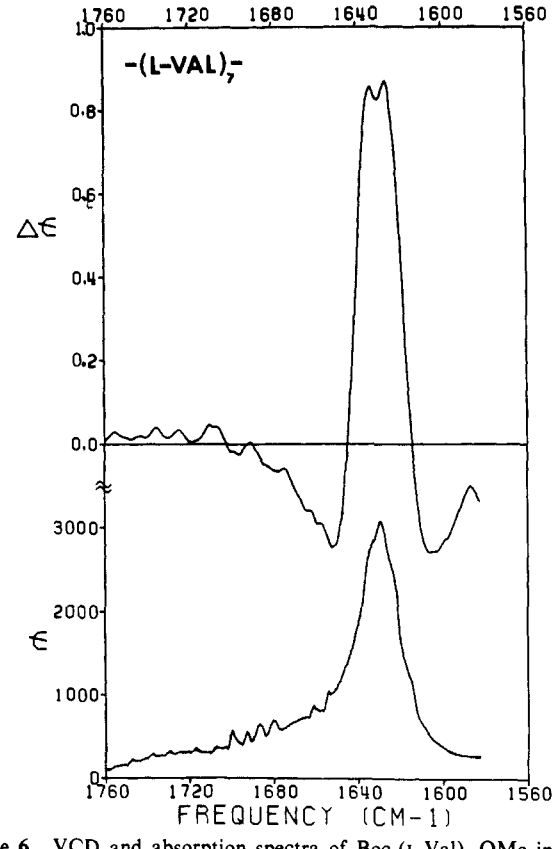

Figure 6. VCD and absorption spectra of Boc-(L-Val)$_7$-OMe in the amide I region [concentration ≃2.4 mM in TFE, path length 0.02 cm, resolution 14 cm^{-1}, time constant 30 s, four scans averaged].

Solution Studies. Due to interference by the solvent (TFE or HFIP) absorption, only the amide I band could be studied for solution samples. The resulting spectra in cloudy, nearly saturated TFE solution are shown in Figure 6 and 7 for the (L-Val)$_7$ and

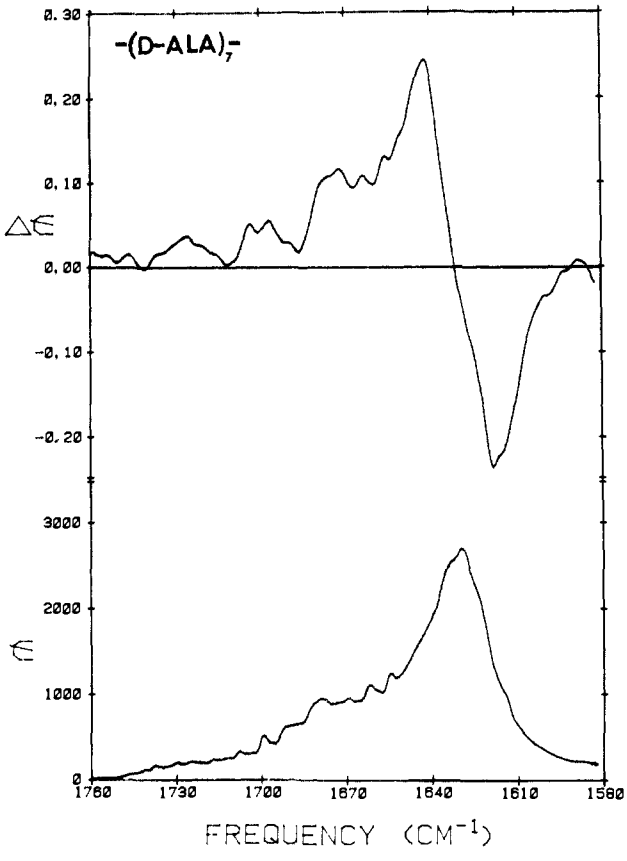

Figure 7. VCD and absorption spectra of Boc-(D-Ala)$_7$-OMe in the amide I region [concentration 3.7 mM in TFE, path length 0.02 cm, resolution 14 cm^{-1}, time constant 30 s, six scans averaged].

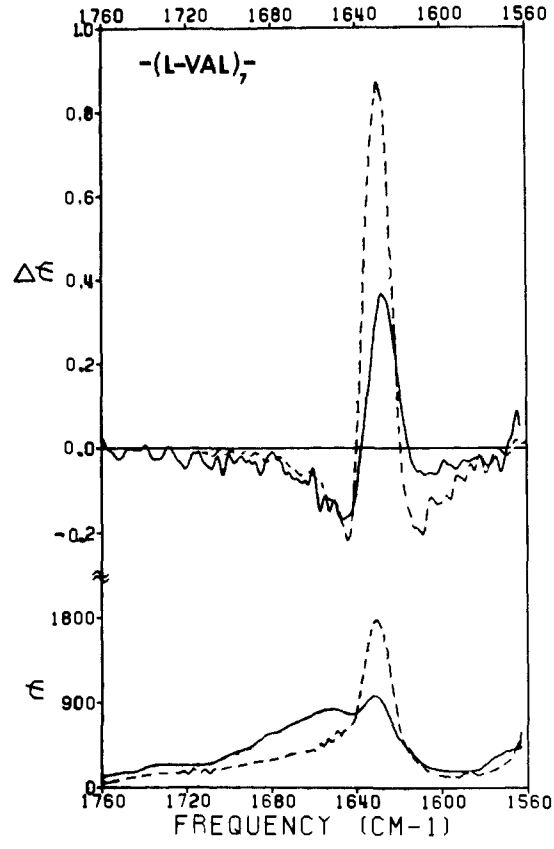

Figure 8. VCD and absorption spectra in the amide I region of Boc-(L-Val)$_7$-OMe in HFIP/TFE solvent mixtures: (---) (Val)$_7$ in a 10% mixture of HFIP/TFE, concentration 5.3 mM; (—) (Val)$_7$ in a 30% mixture of HFIP/TFE, concentration 11 mM. Other conditions: path length 0.02 cm, resolution 12 cm^{-1}, time constant 10 s, two scans averaged.

(D-Ala)$_7$ oligomers, respectively. Both gave strong, peaked absorption near 1630 cm^{-1}, indicative of β-structure formation. The solution (L-Ala)$_6$ gave results similar to that of (D-Ala)$_7$ with the exception that the VCD sign was, of course, opposite. The (L-Leu)$_7$ and (L-Nva)$_7$ samples prepared were clear and unsaturated. These both gave only broad absorption peaking near 1660 cm^{-1} and very weak, broad, noisy VCD that we do not feel is reproducible. This shifted absorption would be characteristic of a random-coil type structure and probably is a result of the oligomers being too dilute to force cooperative intermolecular hydrogen bonding. The (D-Ala)$_7$ sample also gave some absorption and VCD at $\simeq$1680 cm^{-1} that could be indicative of an antiparallel structure.[29] However, since the absorption as well as the VCD appear to have excess noise and since these are urethane-blocked oligomers,[16,17,19,30] any conclusions would be unwarranted as to which chain orientation (either parallel or antiparallel) of β-sheet is dominant.

In the solvent-titration experiments, addition of HFIP to the TFE solutions caused a decrease in the absorbance at 1630 cm^{-1} and a collateral growth of a broad band centered at 1660 cm^{-1}. Spectra for 10 and 30% HFIP mixtures are illustrated in Figure 8. In the cases where we used a nearly saturated TFE/HFIP solution, the $\Delta\epsilon/\epsilon$ values obtained at $\sim$1630 cm^{-1} did not vary significantly with change of solvent, but instead ϵ and $\Delta\epsilon$ both decreased together at that frequency. The band shape at higher HFIP concentration begins to distort from the symmetric (−, +, −) pattern of Figure 6. The above behaviors are consistent with there being a mixture in solution of random-coil and β-structures. In an additional experiment, mixing a saturated TFE solution with an HFIP solution in a 1:1 ratio, no VCD was seen and the absorption became quite broad, peaking at $\sim$1659 cm^{-1}. A weak, but detectable, shoulder remained near 1630 cm^{-1} in absorption. These final changes are probably due, at least in part, to dilution effects since the HFIP was substantially unsaturated. Hence, at 1:1 it is reasonable that $\Delta\epsilon/\epsilon$ should apparently change since the saturation condition is lost.

In general, sample preparation for these oligomers so that they maintain a β-structure in solution is somewhat difficult. At very low concentrations, the amide I IR absorption is broad and may indicate a randomly coiled structure; at high concentrations, the sample precipitates. Our resulting "cloudy" solutions are presumably not ideal for VCD study. However, they appear to be the best compromise available for study of solution-phase β-structure VCD on relatively small molecules. It is known that dilution[16,19] and extended time[31] in solution break up the β-structure. This is the probable cause of loss of VCD activity under these same conditions.

The temperature variation results for the (L-Val)$_7$ oligomer in TFE are summarized in Figure 9. The noise level in terms of $\Delta\epsilon$ in these plots is $\sim$0.1–0.2. The absorption shows growth of a broad band at $\simeq$1665 cm^{-1} with increasing T and a decrease in ϵ of the band at 1630 cm^{-1}. Our experimental conditions, unfortunately, did not permit accurate measurement of the change in ϵ. These absorption changes are paralleled by a faster decrease in $\Delta\epsilon$ as T increases from 40 to 65 °C. Comparative spectra at 21.0 and 58.5 °C are shown in Figure 9. The trend in $\Delta\epsilon/\epsilon$ is that of being roughly constant over 20–40 °C ($\Delta\epsilon/\epsilon \sim (3\text{–}4) \times 10^{-4}$) and showing a gradual decline over 40–65 °C to about twice the $\Delta\epsilon/\epsilon$ detectability limit ($\sim 5 \times 10^{-5}$) for this experiment. Other experiments we have attempted indicate that this final state is concentration dependent. Band-shape changes at various temperatures were not greater than the fluctuation in base line ($\sim$ ±20% of the low-temperature signal). The above results are also consistent with a mixture of randomly coiled structures and β-

(29) Miyazawa, T.; Blout, E. R. *J. Am. Chem. Soc.* **1961**, *83*, 712–718.
(30) Toniolo, C.; Bonora, G. M. In *Peptides: Chemistry, Structure, and Biology*; Walter, R., Meienhofer, J., Eds.; Ann Arbor Science: Ann Arbor, 1975; pp 145–150.

(31) Toniolo, C.; Bonora, G. M., unpublished observations.

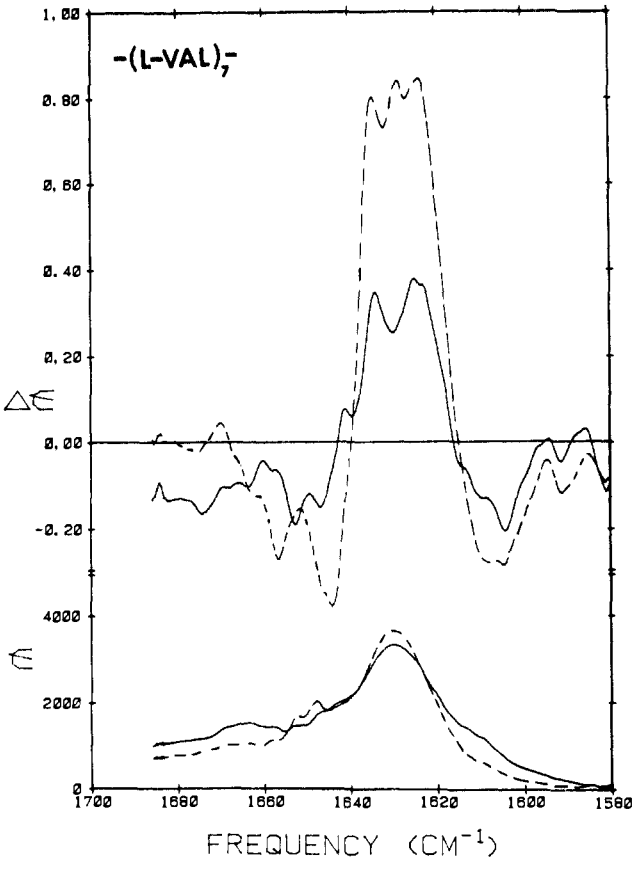

Figure 9. VCD and absorption spectra for Boc-(L-Val)$_7$-OMe in TFE (concentration 2 mM, path length 0.02 cm) in the amide I region: at 21 °C (—); at 58.5 °C (---). Other conditions: resolution 12 cm^{-1}, time constant 10 s, two scans averaged.

structures being present at elevated temperatures. However, loss of VCD clearly precedes loss of 1630-cm^{-1} absorption. The ramifications of this are discussed below.

Discussion

As the plots in Figure 4 clearly show, the VCD film data previously reported[10] for the (L-Ala)$_n$ series are not unique in having $\Delta A/A$ go through a maximum with increasing chain length while coincident with formation of a β-structure. The longer aliphatic side chains represented by Nva, Val, and Leu apparently make it harder to form β-type hydrogen bonds and thus delay the first structural transition to $n = 5$ or 6 as opposed to $n = 4$ in (L-Ala)$_n$. The second such transition (Figure 4) is also delayed, to $n \simeq 7$, for these systems (Val and Nva). The longer chains of Nva and Leu do not seem to yield particularly correlated VCD vs. n results, but, apparently, Leu has less ease of β-formation than do the others. However, as compared to (L-Ala)$_n$, all of the oligomers in this study, having larger side chains, have less stable β-forms for the same value of n. The two structural transitions seen in these $\Delta A/A$ vs. n plots indicate that previous use of just the amide I IR absorption frequency or even of the VUV CD is insufficient to monitor all of the various structural phases occurring in these blocked linear homooligopeptides in the solid state. Clearly, we are seeing at least three different structural types in (L-Ala)$_n$, (L-Nva)$_n$, and (L-Val)$_n$. One interpretation of our data is that these three correspond to (1) disordered structures, (2) the onset of randomly aligned β-type hydrogen bonding, and (3) the formation of fully developed β-structures as n is increased.

Additionally, it may be noted that, in our (L-Ala)$_n$ study,[10] definite trends were seen in the VCD zero-crossing frequency as compared to the peak absorption frequency, while in the cases presented above that is not as evident. We feel this is merely due to signal-to-noise considerations and the difficulty of preparing consistent films of these larger side-chain oligomers. In this sense, the $\Delta A/A$ values prove to be much more valuable and sensitive for monitoring conformational change.

The β-branched Val side chain does give rise to a three-featured band shape for the VCD that is apparent in both film and solution spectra. It is interesting to note that the (L-Val)$_7$ has also been proposed to have the unusual parallel β-structure.[17,19,20,32,33] In this case we would expect the parallel and perpendicular polarized amide I bands to overlap in the 1630-cm^{-1} region.[29] This overlap could give rise to multiple VCD bands. However, the mismatches and end effects that are predominant in a short oligopeptide could also lead to additional bands, and side-chain branching could affect the degree of chain mismatch in a β-structure for a given length oligomer. (We do not understand why the (L-Val)$_7$ film does not share this unusual line shape that it evidences in solution.)

On the other hand, for (D-Ala)$_7$, which is expected to be in an antiparallel β-structure,[17,19,20,32,33] we should have a VCD band (parallel polarized) at $\sim$1690 cm^{-1} that balances out the 1630-cm^{-1} VCD;[29] but we do not see very convincing evidence for such a feature. Only a small absorption shoulder is seen, which has been discussed above. This is not qualitatively different from that found for the other oligomers, e.g. (L-Ala)$_6$, and, as previously noted,[27,30] this may be due to the urethane blocking groups. (In polylysine at high pH, known to be an antiparallel β-structure, a negative VCD band is seen at $\sim$1690 cm^{-1} but no balancing band is found at 1630 cm^{-1}.[34]) In the films, both L-Val and D-Ala ($n = 7$) oligomers give similar spectra and have no noticeable features at 1690 cm^{-1}; while in solution the band shapes qualitatively differ, and (L-Val)$_7$ gives rise to a significantly nonconservative band shape. The latter indicates some coupling with other vibrational modes such as the amide II or, possibly, a local mode. Intermode mixing could be a mechanism for the side-chain characteristics to have an effect upon the amide I VCD. In summary, at this time, we cannot definitely state that parallel and antiparallel β-structures can be differentiated by VCD in these oligomers even though they have distinctly different line shapes.

In this paper we have reported the first oligopeptide β-structure VCD spectra in solution. The band shapes of the data in Figures 6 and 7 clearly parallel the film results in Figure 3 (Val) and in our previous work (Ala),[10] thereby adding credence to our technique of the careful use of films for comparative VCD of similar systems. Such nearly saturated, cloudy solutions, as we were forced to use to obtain consistent results, may give rise to scattering phenomena that could lead to artifacts in the VCD. We believe that the consistency of our solution data with repeated sample preparation and with the film data argues against this. It can also be noted that such scattering effects would be substantially different in the IR as compared to that in the ultraviolet and visible.

Contrary to the film results discussed above, the solution data, at first view, appear to be consistent with two independent structural types being in equilibrium. The growth of a broad band near 1650–1660 cm^{-1} with increasing temperature or HFIP concentration is consistent with the added presence of random-coil type oligomers. As expected, this band does not evidence a large contribution to the VCD. Our observation that $\Delta\epsilon/\epsilon$ is approximately constant at 1630 cm^{-1} favors interpretation of the IR and VCD as arising from two independent structures being in equilibrium as opposed to a gradual or stepwise transformation from an ordered to a disordered structure.

However, the above scenario would only be true in the solvent range of 0–30% HFIP and at temperatures below 40 °C. At temperatures of 40–65 °C, $\Delta\epsilon/\epsilon$ clearly decreases at 1630 cm^{-1} while a significant absorption band remains (Figure 9). A similar phenomenon appears to occur upon dilution. This implies that the magnitude of the observed VCD is a measure of the integrity

(32) Chou, K.-C.; Nemethy, G.; Scheraga, H. A. *J. Mol. Biol.* **1983**, *168*, 389–407.
(33) Chou, K.-C.; Nemethy, G.; Scheraga, H. A. *Biochemistry* **1983**, *22*, 6213–6221.
(34) Keiderling, T. A.; Yasui, S. C.; Sen, A. C.; Toniolo, C.; Bonora, G. M. In *Peptides, Structure and Function, Proceedings of the 9th American Peptide Symposium*; Deber, C. M., Hruby, V. J., Kopple, K. D., Eds.; Pierce Chemical: Rockford, IL, 1985; pp 167–172.

of the β-structure formed. As this melts with increasing temperature, many intermolecular hydrogen bonds might remain in a significantly less ordered intermediate structure. These could give rise to the lower energy (1630-cm^{-1}) amide I bands seen. Some oligomers would eventually lose all memory of the original β-structure and could be in a randomly coiled conformation. Such a two-step structural transition would result in faster loss of VCD (correlated to inter-amide coupling) than absorption at 1630 cm^{-1} (correlated to β-type hydrogen bonds) as we have observed. In this view, the melting is *not* a cooperative phase transition, which is consistent with the observed gradual loss of $\Delta\epsilon/\epsilon$. Thus, the IR absorption frequency alone is *not* a good measure of the nature of the secondary structure in these compounds. In light of our results, over reliance on IR frequency measurements is probably, in general, unwise for conformational studies.

The deviation of IR and VCD spectra implies that the solution phase could also be viewed as having three structural types; β-structure, random coil, and one or more intermediate phases in contradistinction to our first view (above) of the data. The similarity of these to the film structural types discussed above is open to question.

It should be noted that in solution we probe the conformations of only one oligomer while in the solid state we attempt to compare conformations of several different oligomers. Hence, the usefulness of such a comparison is probably limited. At this time we cannot state to what extent mixed structures occur in each film sample. We can only propose that there appear to be three structural types. These VCD data also may be strongly affected by chain length and thus not all relevant to the $(L\text{-Val})_7$ and $(D\text{-Ala})_7$ solution cases. However, the consistency of the solution and film data suggests that the ideas proposed in the previous paragraphs are not totally irrelevant.

In summary, our results indicate that combining VCD with IR and CD results can lead to new insight into polypeptide and oligopeptide structural transitions. It is clear from the above discussion that the traditional method of using IR frequencies to determine secondary structure is limited in information content. In particular, one typically wants to know whether an extended β-structure has formed or not. This appears to be most detectable by VCD or CD techniques. The IR frequencies alone appear to sample the much more local phenomenon of interchain hydrogen bonding and, as such, can lead to premature conclusions as to structural integrity. From the results presented in this paper, added structural complexity beyond that previously proposed is evident in both the solid and solution phases of the oligomers studied. It is hoped that our work will stimulate future studies to be more carefully analyzed with respect to peptide conformation.

Acknowledgment. U.N. and T.A.K. acknowledge financial support from the National Institutes of Health (Grant GM-30147) and the National Science Foundation (Grant CHE81-04997) for this work.

Resonance Raman Study of Oxyhemerythrin and Hydroxomethemerythrin. Evidence for Hydrogen Bonding of Ligands to the Fe–O–Fe Center

Andrew K. Shiemke, Thomas M. Loehr, and Joann Sanders-Loehr*

Contribution from the Department of Chemical, Biological, and Environmental Sciences, Oregon Graduate Center, Beaverton, Oregon 97006-1999. *Received October 16, 1985*

Abstract: Hydrogen bonding in the ligand binding site of the respiratory protein hemerythrin has been investigated by resonance Raman spectroscopy. Evidence for hydrogen-bond interactions between the oxo bridge of the Fe–O–Fe moiety and the exogenous ligand has been found for both oxy- and hydroxomethemerythrin. In the latter case peaks are observed at 492 and 506 cm^{-1} that shift upon ^{18}O bridge substitution to 477 and 491 cm^{-1}, respectively. These are assigned as ν_s(Fe–O–Fe) modes of two distinct Fe–OH conformations: the cis conformer nas an intramolecular hydrogen bond between the bound hydroxide and the oxo bridge that is lacking in the trans conformer. This proposal is supported by the observation of a temperature-dependent equilibrium between the conformers, with the cis conformer becoming more prevalent at low temperature as indicated by the increased intensity at 492 cm^{-1} relative to 506 cm^{-1}. The variation in the intensity as a function of temperature yields a ΔH° of −0.4 kcal/mol for the trans to cis conversion, consistent with the formation of a weak intramolecular hydrogen bond. The low frequency of ν_s(Fe–O–Fe) for *cis*-hydroxomethemerythrin relative to that of other methemerythrins is caused by weakening of the bridge bonds when the oxo group acts as a hydrogen-bond acceptor. A similarly low ν_s(Fe–O–Fe) frequency of 486 cm^{-1} is observed for oxyhemerythrin, indicating that the bound hydroperoxide ligand also has the ability to hydrogen bond to the oxo bridge. This hydrogen bond is considerably stronger than that of the hydroxide adduct such that only a single ν(Fe–O–Fe) peak is observed for oxyhemerythrin between 90 and 300 K. This peak undergoes a shift of +4 cm^{-1} in D_2O, an effect specific to oxyhemerythrin, owing to a weakening of the hydrogen bond upon deuterium exchange. An effect of deuterium exchange is also observed for *cis*-hydroxomethemerythrin, although in this case the shift is due to coupling between ν_s(Fe–O–Fe) and the Fe–O–D bending vibration. An additional peak located at 565 cm^{-1} in hydroxomethemerythrin is assigned as the Fe–OH stretch on the basis of its shift to 538 cm^{-1} in $^{18}OH_2$. The relative intensity of this peak is independent of temperature, indicating that hydrogen bonding has little or no effect on the Fe–OH vibration.

Hemerythrin is a nonheme iron-containing respiratory protein found in many marine invertebrates. The coelomic protein from the sipunculid *Phascolopsis gouldii* has an octameric quaternary structure, as does the protein from most other sources.[1] Each protein monomer contains one dioxygen binding site involving two iron atoms that, in the deoxy form of hemerythrin, are in the ferrous state.[1,2] After the dioxygen is bound, the iron atoms are oxidized to the ferric state with concomitant reduction of O_2 to peroxide, resulting in the formation of oxyhemerythrin.[2-5] An

(1) (a) Sanders-Loehr, J.; Loehr, T. M. *Adv. Inorg. Biochem.* **1979**, *1*, 235-252. (b) Klotz, I. M.; Kurtz, D. M., Jr. *Acc. Chem. Res.* **1984**, *17*, 16-22. (c) Wilkins, R. G.; Harrington, P. C. *Adv. Inorg. Biochem.* **1983**, *5*, 52-85. (d) Sanders-Loehr, J. In *Frontiers in Bioinorganic Chemistry*; Xavier, A. V., Ed.; VCH Publishers: Weinheim, 1986; pp 574-583.

(2) Sanders-Loehr, J.; Loehr, T. M.; Mauk, A. G.; Gray, H. B. *J. Am. Chem. Soc.* **1980**, *102*, 6992-6996.

(3) Garbett, K.; Darnall, D. W.; Klotz, I. M.; Williams, R. J. P. *Arch. Biochem. Biophys.* **1969**, *135*, 419-434.

(4) Dunn, J. B. R.; Shriver, D. F.; Klotz, I. M. *Proc. Natl. Acad. Sci. U.S.A.* **1973**, *70*, 2582-2584.

0002-7863/86/1508-2437$01.50/0